

Characteristics of a permanent magnet low power Hall thruster

IEPC-2009-083

*Presented at the 31st International Electric Propulsion Conference,
University of Michigan • Ann Arbor, Michigan • USA
September 20 – 24, 2009*

A. Leufroy , T. Gibert and A. Bouchoule
GREMI Laboratory, Orléans University & CNRS, 45067, ORLEANS Cedex2 , FRANCE

Abstract: A low power Hall Effect Thruster (HET), based on a flexible permanent magnet design, was presented at Heraklion conference¹. The operation range, the performances and some physical characteristics of this thruster, hereafter called PPI, have been investigated and are reported in the present paper. After a short introduction, the part II of this paper presents the main features of the PPI thruster, its three successive magnetic versions and their operation ranges when investigated in the small size, high pressure, facility of the GREMI laboratory and operated in the large scale, low pressure, national facility PIVOINE, for thrust measurements.

The current-voltage characteristics and thrust performances are reported in Part III. The thruster current exhibits strong oscillations in GREMI conditions, in the usual ten's of kilohertz frequency range, while a moderate level of current fluctuations is observed in PIVOINE conditions. While current-voltage discharge characteristics suggest a reasonably high ionization efficiency, rather low thrust efficiencies and ISP's have been obtained.

Some physical investigations of thruster and plume are described in Part IV. The plume divergence in GREMI is reduced in comparison with PIVOINE conditions, in agreement with previous studies of facility pressure effects. Time of Flight (TOF) phenomena were observed in oscillating regimes through simultaneous records of the thruster discharge current and of the collector current of an RPA. These TOF data suggest significant contributions of Xe⁺⁺ ions in the plume. A small antenna, located near the channel exit, evidenced instabilities in the range of 5-10 MHz which are observed at a peculiar phase of the low frequency current fluctuations observed in PIVOINE conditions.

The conclusive part V summarizes the main throughputs of this work .

Nomenclature

CPAT = « Centre de Physique et Application des Plasma » (*research laboratory of CNRS and Toulouse University*)
GDR = “Groupement de Recherche » (*coordinated research organisation*)
GEMAC = “Groupe d’Etudes de la matière Condensée” (*research laboratory from CNRS and Versailles-St Quentin University*)
GREMI = “Groupe de Recherche sur l’Energétique des Milieux Ionisés”(*research laboratory from CNRS and Orléans University*)
HET = “Hall Effect Thruster”
ICDEF = « Ion Current *total* Energy Distribution Function »
PPI = “petit propulseur innovant” (*small innovative thruster*)
RPA = « Retarding Potential Analyzer »
TOF = “Time Of Flight”
W = Watts

I. Introduction

THIS paper describes technical and physical studies devoted to a Hall Effect Thruster (HET) operated in the 50-300 W domain with a magnetization achieved by using permanent magnets. Even if the use of permanent magnets for HET's was already reported in seventies², the evolution of magnetic materials, and the interest for electric propulsion at reduced thrust, lead more recently to many studies where permanent magnet circuits were involved in new thruster concepts^{3,4}. They were used for magnetization of a PPS 100 ML thruster, by the same team of GEMAC laboratory who designed the magnetic field of the thruster involved in the present study, with performances similar to those obtained with conventional coils magnetization⁵.

The goals of this work was to demonstrate that a permanent HET structure can support the thermal constraints of an HET, to gain insights on the possible magnetic versatility offered by the assembly of very small size magnets, called hereafter mini-magnets, and finally to test the performances of this first hand magnetic design. Besides the magnetic circuit realization, the thruster itself was designed and built by GREMI laboratory and the PPI thruster was presented in details at the 2008 Space Propulsion Conference¹ together with very preliminary tests of operation.

The mini-magnet concept has been used in this study to make a comparison between three PPI versions having the same magnetic topology but different magnetic field intensities. Limited performance values have been obtained in the PIVOINE facility, but the thermal stability and the overall behavior of the thruster are encouraging for further improvements. Besides performance considerations, the interest of such reduced power device concerns physical studies. Physical investigations of PPI presented in this paper underline this aspect. Most of them were achieved in the smaller size, and higher working pressure, GREMI facility.

II. PPI thrusters and operating conditions involved in this study

The aim of this part is to give an overview both on the three successive versions of the PPI involved in this study and on the operating conditions used in the two facilities mentioned above.

II 1 : A magnetically flexible design based on mini-magnets

The magnetic circuit of the PPI HET's was based on preliminary simulations achieved in the CPAT laboratory, by using the hybrid code^{see ref 6} developed in the team of J-P. Boeuf. This magnetic circuit was built by the GEMAC laboratory by using exclusively permanent magnets and a magnetic topography very close to the simulation model has been achieved. Details on PPI structure can be found in ref 1 and a short presentation is given below.

The main overall structure of the PPI, technically designed and built by GREMI laboratory, is shown on Fig 1.

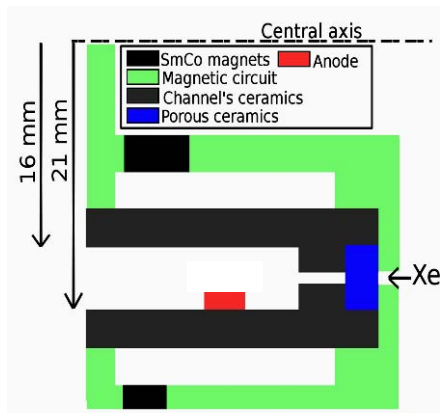


Fig 1 structure of PPI thruster

The Xenon flow enters the channel through a porous ceramics plate. The anode is an annular ring located in the external ceramics, near the channel bottom.

The PPI magnetic field is obtained with arrays of small size (L and Φ in the mm range) SmCo mini-magnets arranged in external and internal rings, as shown on figure 2 (176 magnets external, 54 magnets internal).

When replacing a fraction of mini-magnets by stainless-steel mini-cylinders, it was possible to decrease the intensity of the PPI magnetic field below its maximal value, without changing its magnetic topography. Three PPI versions have been realized with radial magnetic fields shown on figure 3. They were called referred as PPI H, PPI M and PPI L, corresponding to decreasing values of magnetic field.

The Xenon flow enters the channel through a porous ceramics plate. The anode is an annular ring located in the external ceramics, near the channel bottom.

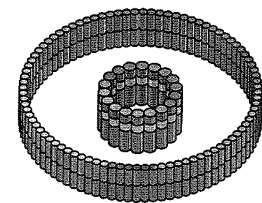


Fig 2 : SmCo mini-magnets of external and internal rings

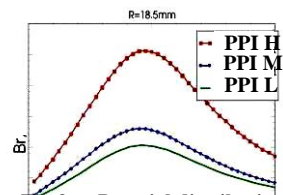


Fig 3 : Br axial distribution of the three PPI versions

One of the interests of permanent magnets is to reduce the volume, usually required by coils, to achieve a given magnetic flux. This peculiarity allowed the installation of copper cylinders for heat transfer to the bottom copper flange of the thruster structure. A copper cylinder can be used for heat release from this bottom flange by radiative cooling. The figure 4 shows PPI running without radiator and figure 5 shows the PPI equipped with radiation cooling.

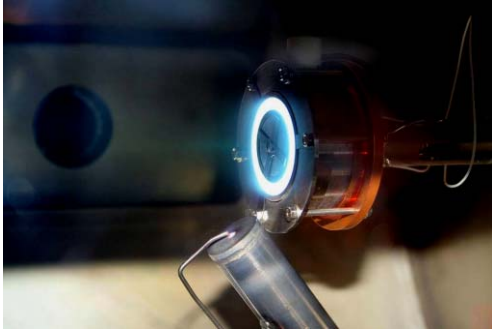


Figure 4 : PPI thruster operated in GREMI facility without radiation cooling

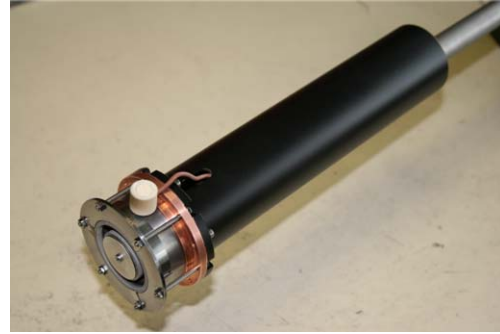


Figure 5 : PPI thruster equipped with radiation cooling

Three temperature data were available during PPI tests, as shown on the drawing of Fig 5bis . These data were required in the first tests for thermal safety of mini-magnets.

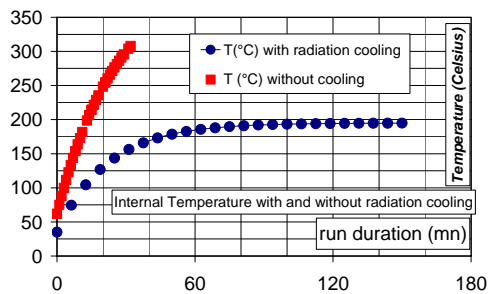


Figure 6 : temperature increases during a run of PPI M operated at 200W with & without cooling

The figure 6 illustrates the effectiveness of this radiation cooling by comparing the elevation of the internal temperature of PPI M operated at 200 Watts as function of run duration. As the maximum allowed value was near 300 °C , the run without cooling is reduced to less than 30 mn while a permanent and safe operation was available with cooling.

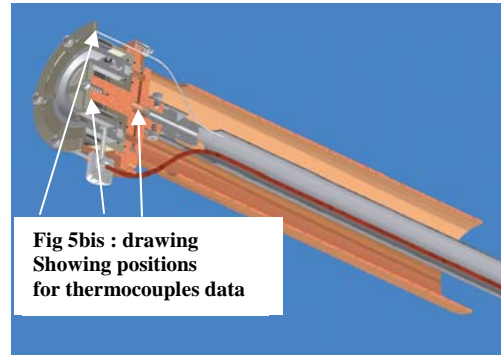


Fig 5bis : drawing Showing positions for thermocouples data

II 2 Facilities and operating conditions

Performances of PPI M and PPI L were studied at very low pressure operating conditions ($< 8 \cdot 10^{-6}$ mbar) in the PIVOINE-2G facility⁷ after a special improvement and calibration of the PIVOINE thrust balance in order to obtain reliable data in the thrust range of 1-20 mN.

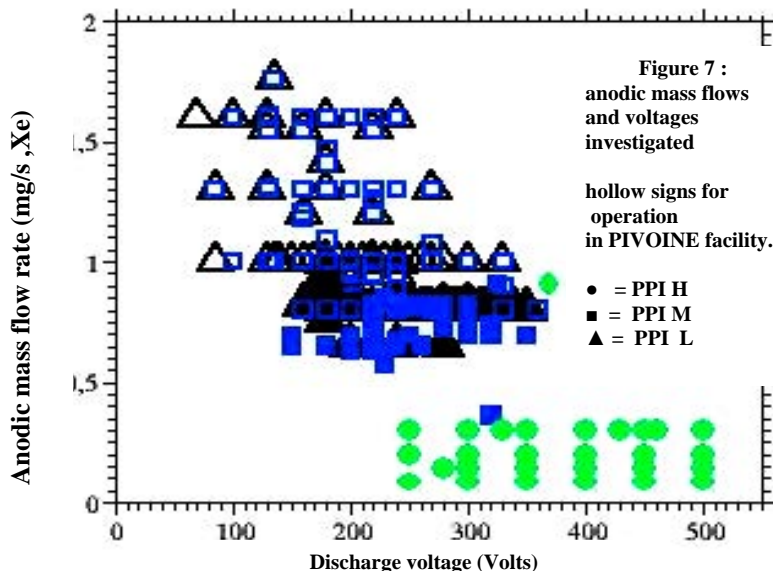


Figure 7 : anodic mass flows and voltages investigated
hollow signs for operation in PIVOINE facility.
● = PPI H
■ = PPI M
▲ = PPI L

Electrical and some physical characteristics of PPI H-PPI M and PPI L were obtained in the smaller GREMI vacuum vessel⁸ (1m length, 0,5 m diameter, 4000 l/s pumping rate) where the operating pressure was as high as $1.5 \cdot 10^{-4}$ mbar for a total Xenon flow of 1.6 mg/s .

The mass-flow/voltage operating domains used for PPI studies are shown on figure 7, where the facilities conditions are specified (empty symbols: PIVOINE, filled symbols: GREMI) as well as PPI versions (circles =PPI H, squares = PPI M, triangles = PPI L).

A reliable hollow cathode of the thruster SPT100ML (from MIREA Institut) was always used in this work, in order to avoid any cathode problems. The consequence is that the xenon cathodic

flow was at least 30% of the anodic one. The thrust efficiencies reported in the paper are related only to the xenon flow injected at the bottom of the channel, called below, as usual, the anodic gas flow.

III. Performances and electrical characteristics

Two significant differences of electrical characteristics were observed in GREMI and PIVOINE operation. The first one concerns the operating domain, where higher mass flows are generally required in PIVOINE conditions for achieving a stationary regime. The second one concerns the discharge current regime with strong oscillations observed in GREMI facility and rather low level fluctuation regime observed in PIVOINE operation.

The performance data obtained in PIVOINE are given in the first section. The comparison of thruster characteristics obtained in GREMI and PIVOINE conditions will be found in the second one.

III 1 : Performances recorded in PIVOINE facility : PPI M and PPI L

An extended set of data, for anodic mass flow rates of 0.8 to 1.6 mg/s, is shown below for the PPI M thruster : current-voltage characteristics (Fig. 8), thrust data (Fig. 9) and ISP (Fig. 10).

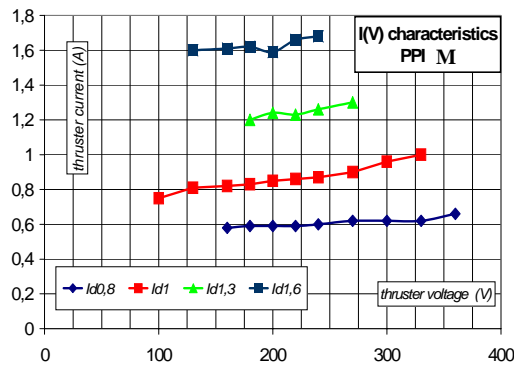


Figure 8 : I(V) characteristics of PPI M in PIVOINE facility. Curves label correspond to mass flow rates of 0.8, 1,0, 1.3 and 1.6 mg/s

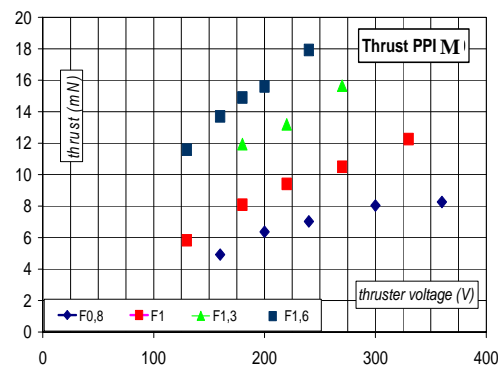


Figure 9 : thrust data for PPI M in PIVOINE facility. Same mass flow rate labels

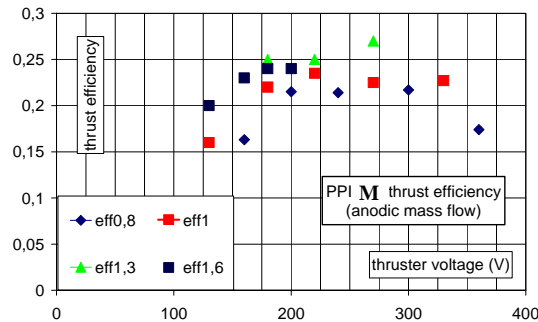


Figure 10 : PPI M thrust efficiency related to anodic flows with the same labels

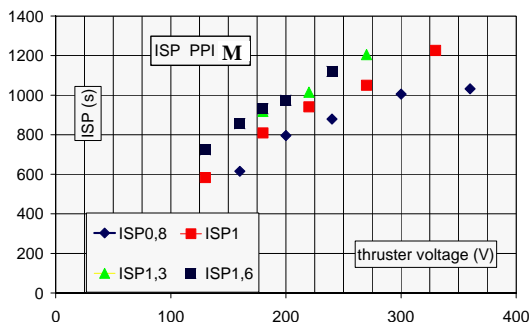


Figure 11 : PPI M ISP

As can be seen, this PPI thruster leads to lower performances than reported in the literature, in the same range of mass flow and electrical power ^{eg 9,10}. But these results are nevertheless interesting ones, recalling that PPI represents a “first hand magnetic design” and that the thermal concept leads to stable operation, even after exploring electrical power as high as 400 Watts.

Similar data have been acquired in PIVOINE facility for the PPI L thruster. The figure 12 shows that it’s performances are a little bit below the PPI M ones.

The robustness of the PPI design was evidenced by recording again, in the PIVOINE facility, the performances of the PPI M after about hundred hours of overall operation in various conditions. The figure 13 shows that similar performances were obtained, close to the ones recorded one year before.

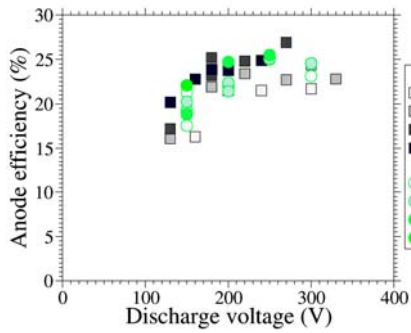


Figure 12 : right
Thrust efficiencies of PPI M (■) and PPI L (●)

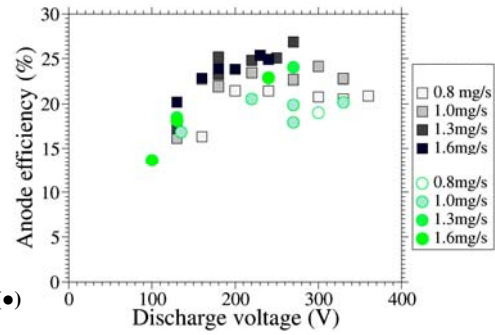


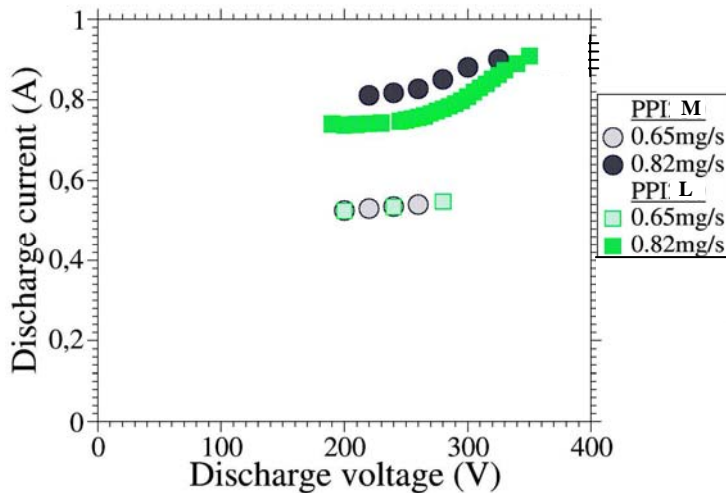
Figure 13 left
thrust efficiencies of PPI M recorded in 2008 (■) and 2009 (●)

III 2 : PPI's characteristics when operated in GREMI facility

Studying thrusters in this small scale facility has the significant interest to be much less expensive and much more flexible. At first approximation, the perturbation related to facility pressure operation could be estimated by comparing the Xe flow injected into the channel from the facility chamber to the Xe anodic gas flow. Pertinent values for this evaluation are given by PPI operation at an anodic gas flow of 1.3 mg/s, a cathodic gas flow of 0.6 mg/s and a working pressure of $1 \cdot 10^{-4}$ mbar. Taking into account these data, the channel inflow from the facility represents less than 1 % of the anodic Xe flow.

A. Current-voltage characteristics obtained for PPI M and PPI L in the GREMI facility

The highest magnetic field version, PPI H, required both high mass flow rates and high voltages for sustained operation. With power up to 500 watts, this thruster was always out of the security domain for thermal accommodation of long duration runs ($< 5-10$ mn). Nevertheless these runs were long enough to record physical properties such as current waveforms. Permanent runs were obtained for the two other PPI's versions, sustaining power levels up to 300 Watts when using the radiative cooling.



I(V) characteristics of PPI M and PPI L, obtained with the same mass flow rates, are shown on figure 14. The PPI L thruster current is close to, but lower than, the PPI M' current for the same operating parameters. But it's thrust efficiency, measured in PIVOINE facility, is lower than for PPI M. These data suggest that PPI L is less efficient in terms of ionization efficiency.

Figure 14

I(V) characteristics of two versions of PPI
For two anodic gas flows are indicated
○ = PPI M
□ = PPI L

B. Facility effects on current-voltage characteristics

A stable permanent regime was obtained in the PIVOINE facility for higher mass flow rates than observed in GREMI facility.

The I(V) characteristics of PPI L, obtained for mass flows of 0.8 in GREMI facility and 1 mg/s in PIVOINE facility, are shown on figure 15. The small dots curve is a derivation of a I(V) characteristic in GREMI for 1 mg/s, assuming that the current is, at first approximation, proportional to the mass flow rate in the interval 0.8-1,0 mg/s.

The thruster current was lower, by 5-10%, in PIVOINE conditions for all comparisons made during this work.

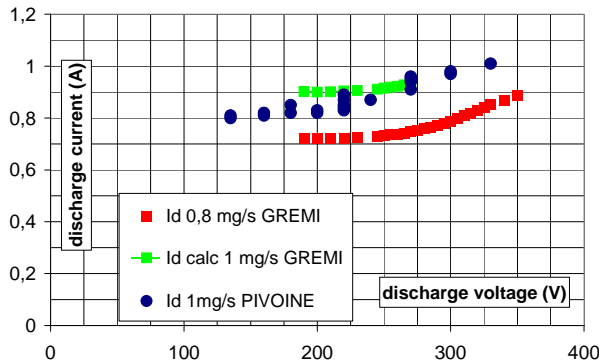


Figure 15 : I(V) characteristics for the thruster PPI L obtained in PIVOINE facility at 1,0 mg/s anodic gas flow and in GREMI facility at 0.8 mg/s.
(see text for the extrapolated curve GREMI at 1,0 mg/s)

The Xenon gas flow injected from the facility towards the thruster channel is less than 1 percent of the anodic gas flow and cannot explain the difference. The Xe atomic density in the region between cathode and channel is much higher in GREMI facility than in PIVOINE facility. The observed increase of current in GREMI facility could be related to the corresponding enhancement of the electron mobility across magnetic lines in this region, and near channel output.

As the I(V) characteristics differ by less than 10% in GREMI and PIVOINE conditions, the PPI investigations achieved in GREMI facility conditions appear useful for studies of thrusters in this 50-300 Watt , 0.5-1.6 mg/s domain.

IV. Physical insights on PPI thruster's features

The studies presented in this paper concern angular features of PPI thruster plumes obtained in GREMI and PIVOINE conditions and also the low frequency (tens of kHz) and the high frequency (5-10 MHz) fluctuations and instabilities observed in GREMI and/or PIVOINE conditions.

IV 1 : low frequency current instability and time averaged plume features

The PPI's current regime observed in GREMI facility was almost always a strongly oscillating one with frequencies in the familiar range of few ten's kHz. In contrast, limited level fluctuating regimes were observed with similar frequencies in PIVOINE conditions. The plume divergence showed also significant differences between GREMI and PIVOINE operation. While I(V) characteristics are similar, these two aspects underline the impact of facility conditions on thruster behaviour.

A : pulsating and fluctuating current regimes in GREMI and PIVOINE facilities

The most significant difference of PPI's features when operated in the two facilities concerns the discharge current regime.

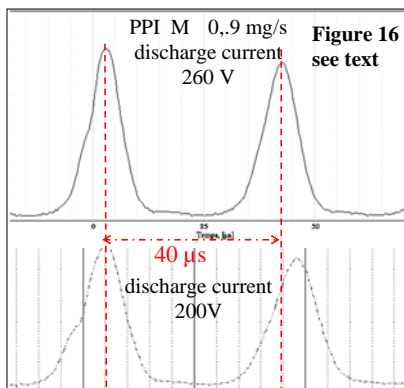


Figure 16 see text

Burst of current are always recorded in GREMI facility. Figure 16 shows the current pulses obtained for PPI M at the same mass flow (0.9 mg/s) and two discharge voltages. The frequency increases from 23 kHz at 200 V to 25 kHz at 260 Volts. The delay between recordings is short enough to prevent a significant variation of channel temperature and this frequency variation should be related to the width of the current pulse. This width is reduced at higher frequency, suggesting a faster ionizing burst.

In a similar way, the current pulses have a shorter width for PPI H than for PPI M and the breathing frequency is also higher as shown on figure 17 .

The breathing nature of these oscillations was evidenced in many single sweep oscilloscope recordings by the relationship between the time interval between pulses and the current peak amplitude, as can be seen on figure 17 for the PPI H.

The time averaged current in Figure 17 was 1.1 A for the PPI H. The first current high peak value was 3.7 A and the pulse FWHM was 7 µs. It's interesting to compare the amount of gas injected during the very low current

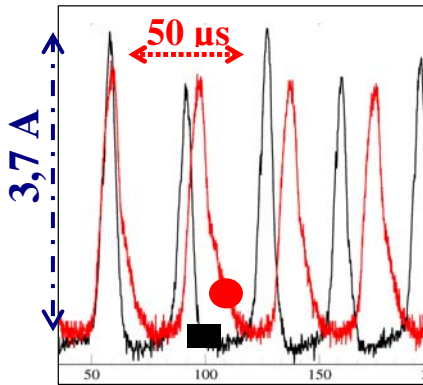


Figure 17 PPI current oscillations recorded for anodic flow 0,95 mg/s and discharge voltage 350 V

● = PPI M ■ = PPI H

is also shown on figure 18. The very high frequency evidenced by this antenna will be examined in details in the next section. Instabilities at an intermediate frequency of 300 kHz are evidenced on the discharge current in this single sweep record. In this frequency domain the most probable interpretation is the so-called ion transit time instability reported also in PPS 100ML thruster¹¹ and predicted in simulations¹².

B : thruster plume : ion energies and divergences

Conventional energy analyzers (RPA), with four grids and aligned holes, were used to record the ion current density energy distribution function (ICEDF) of ions in the plume. Angular distributions of ICEDF were available by moving RPA's along a circle centered at 35 cm from the channel exit center. The RPA grids were facing the local ion beam ejected by the thruster for each angular position.

In the worse pressure conditions of PPI operation the pressure in GREMI facility remains lower than $1.5 \cdot 10^{-4}$ mbar. For Xe^+ ions at kinetic energy of 200 eV, the charge exchange cross-section is of the order of $50 \cdot 10^{-20} m^2$ (ref. 17). The corresponding mean free path is always lower than 0.5 m in GREMI facility and 6 m in PIVOINE conditions. It means that the probability of collisions before RPA entrance can be as high as 50% in GREMI facility and remains fully negligible in PIVOINE conditions.

Records of RPA characteristics in both facilities are shown on Fig. 19 for an axial position and on Fig. 20 for an angle of 20 degrees. These data were obtained with the same PPI thruster operated at the same mass flow rate but at discharge voltages of 240 V for GREMI recordings and 250 V for PIVOINE recordings.

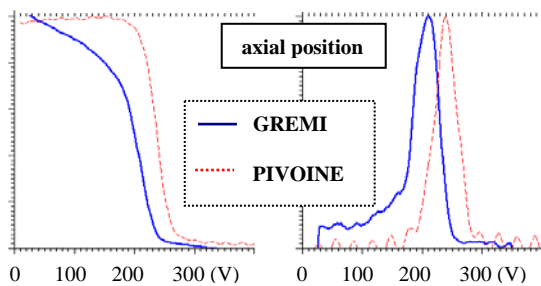


Figure 19 : see text

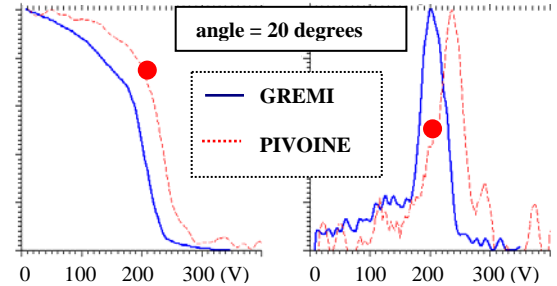


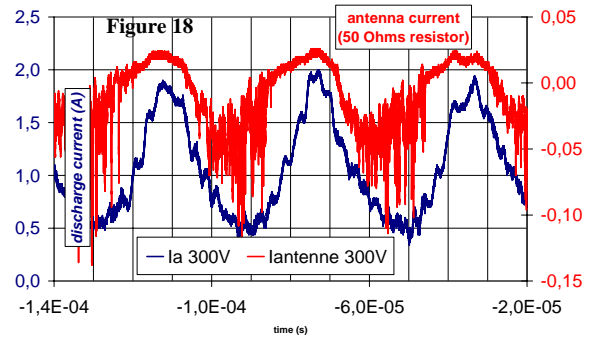
Figure 20 : see text

The ICEDF derived from RPA characteristics have the same apparent width, around 50 eV. The transfer function of these RPA's were characterized by using a mono-energetic ion source and lead to an RPA induced broadening of

period of 26 μs . In the conditions of figure 16 the mass flow was 0.95 mg/s and the Xe injected in the channel during 26 μs represents $1.2 \cdot 10^{14}$ atoms. The corresponding charge, for single charge ions, is $1,8 \cdot 10^{-5}$ Cb. If this charge was delivered in a current burst with same FWHM of 6 μs the corresponding current maximum would be 2,6 Amperes, lower than the real current but the real current involves also electron flow entering the thruster channel. This estimation is in agreement with the common idea that pulsed regimes remain efficient in terms of ionization efficiency. It is also coherent with the similar time averaged currents measured in GREMI and PIVOINE, the current regime being rather quiet in the last one.

The figure 18 illustrates one of the strongest fluctuation regime observed in PIVOINE facility. The low frequency remains close to 25 kHz, as in GREMI conditions, but the RMS value of current fluctuation reaches only 50% of the mean value $\langle I_a \rangle$ equal to 1,1 Ampere.

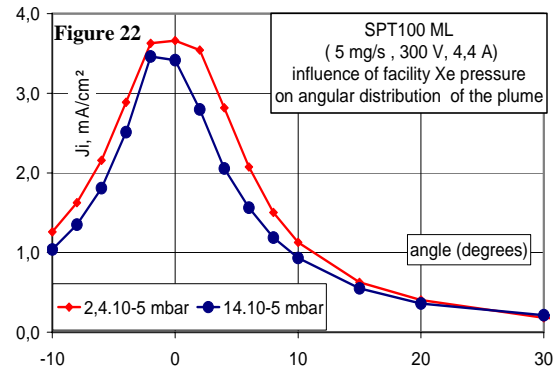
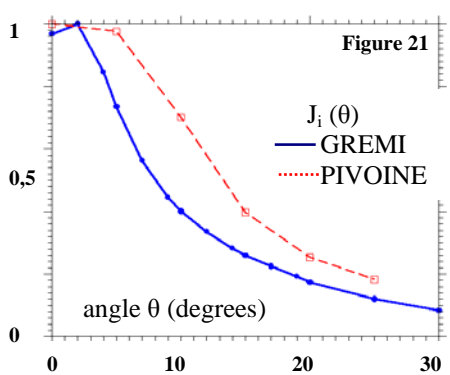
The signal recorded by an antenna located near the plume and close to the channel exit



20-25 eV for ion energies of 200 eV. It means that the plasma potential drop in the main ionization zone is at most 30 Volts.

The RPA determines the total energy of ions as referred to the ground (vacuum vessel) potential. The maxima of the ICEDF are obtained for 210 eV and 240 eV, respectively for GREMI and PIVOINE data. Single charge ions are produced with negligible initial kinetic energy and their total energy corresponds exactly to the local plasma potential of the ionization event. The anode potentials, referred to ground potential, were 249 Volts in PIVOINE and 228 Volts in GREMI. It means that the time averaged potential drop between the anode potential and the main ionization zone is 9-10 Volts in PIVOINE and higher, 18-20 Volts, in GREMI facility.

The angular distribution of the ion plume was only available up to 30 degrees in GREMI operation. A comparison of the angular distributions of the total ion current density, measured in both facilities is shown Fig. 21. As can be seen the plume observed in GREMI conditions is significantly less divergent, in this angular domain. It could be related to the pulsating regime in GREMI conditions, as suggested in other studies in agreement with other As shown on figure 22, less pronounced, but similar effects, were measured when varying the PIVOINE facility



pressure during an SPT100ML run, at fixed operating parameters.

The divergence of the plume measured in PIVOINE, appears consistently higher for PPI than for PPS 100ML : the angles corresponding to half of the current density axial value are respectively 15 and 7 degrees. This significant plume broadening of PPI could lead to a lowering of the PPI thrust efficiency.

The ICEDF of Figs 19 and 20, recorded in PIVOINE facility, suggest the appearance of a low energy contribution when the angle increases. We evaluate this contribution in sharing the ICEDF in two parts : a high energy part for energies higher than indicated by the red dot on figure 20 and a high energy part for the lower energies. The evolution of these two ion current density components is shown on figure 23. It is worth to recall that RPA data represent E_i/q data : double charge ions having a total energy two times higher than single charge ones will be repelled by the same grid voltage. The “low E_i/q ” component can be related to single charge ions or double charge ions, with ionizations achieved in the upstream and lower potential region of the thruster plasma.

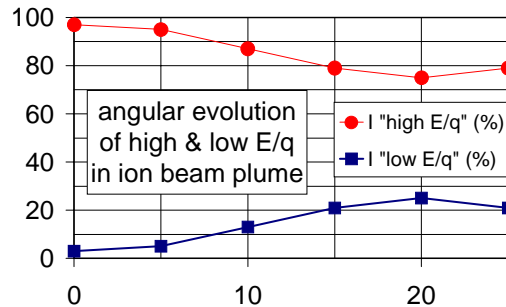


Figure 23
Data derived from ICEDF data
PPI L in PIVOINE, 1 mg/s 250 Volts

IV 2 : Other insights on PPI physical features

The studies reported below concerns the characterization of the high frequencies evidenced on Fig.18 and an evaluation of single/double charge ions contributions derived from TOF data recorded in the pulsating regime of thrusters current.

A : high frequency instability in PPI plasma

The figure 24 shows the shielded wire antenna installed near the exit of PPI thruster. The antenna signal is recorded on a the DC 50 Ω input of a fast sampling scope through a 50 Ω coaxial cable.

Real time high frequency signals, recorded during in the low current period of thruster current fluctuations are illustrated on figure 25 , while a spectrum analysis performed on a rather large time scale of 40 μ s is shown on figure 26.

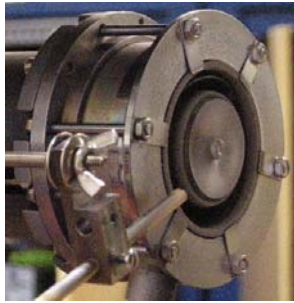


Figure 24

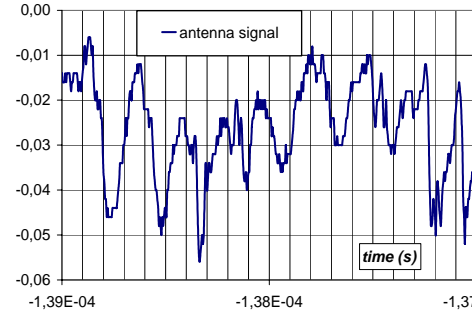


Figure 25

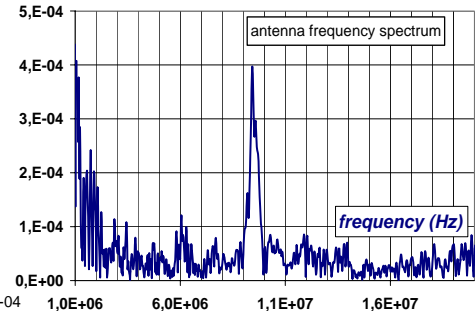


Figure 26

These high frequency instabilities were reported long time ago¹³ and are observed in almost all HET's and detailed studies¹⁴ suggesting their connection with electron transport were reported more recently. It's interesting to note that when looking at PPI instabilities these instabilities are also evidenced.

B : time of flight (TOF) studies of PPI plume

The contributions of Xe^+ and Xe^{++} ions in an PPS 100ML plume were obtained in previous studies by using very short interruptions of anode current. The time resolved RPA collector current revealed these ion contributions by TOF effects¹⁵. The PPI thruster's current, when operated in GREMI facility, was a pulsating one and we tried similar TOF studies by using this spontaneous pulsing regime. Time resolved acquisitions of the collector current of the RPA are shown on Fig. 27 and 28, obtained for a discharge voltage of 240 Volts, a cathode voltage of -10 Volts and a time averaged discharge current of 0,57 Amperes. The ion bursts delivered in the plume are evidenced in these recordings.

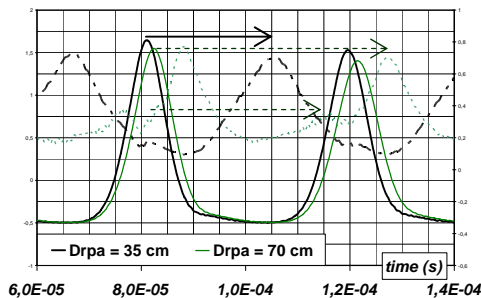


Figure 27

PPI anode current and RPA collector current
Recorded at two distances from thrusters
 thin continuous = anode current
 thin dashed = collector current at 70 cm
 thick continuous = anode current
 thick dashed = collector current at 35 cm

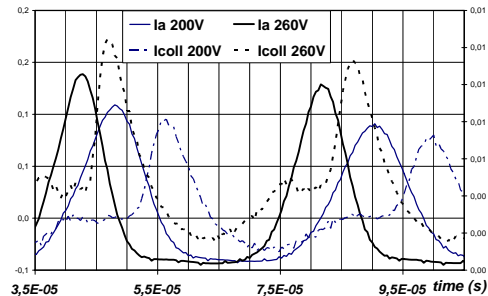


Figure 28

PPI anode current Ia and collector current Ic
(recorded at 70 cm from channel exit) for two
discharge voltages Ud
 thin continuous : Ia for Ud = 200 Volts
 thin dashed ; Ic for Ud = 200 Volts
 thick continuous : Ia for Ud = 260 Volts

The main peak in the RPA collector current is consistent with a contribution of single charge ions. In figure 27 the corresponding travel velocity is the same for the two recordings achieved at 35 and 70 cm from the thruster. This velocity is 15.300 m/s and corresponds to a kinetic energy of 160 eV. The maximum value of the ICEDF was measured by time averaged RPA characteristics and is obtained at 200 eV. It means that the plasma potential in the plume should be of the order of + 40 Volts in these conditions. High values of plasma potential, up to 60 Volts, were previously observed in the same GREMI facility during tests of RPA by using a gridded ion source. They were assigned to the significant, positive, surface potential acquired by large glass windows viewing the ion beam.

The RPA collector signals obtained for two discharge voltage of 200 and 260 Volts are shown on Fig 28. The kinetic energies, derived from the delay between the collector current and the discharge current, are respectively 35 eV lower and 15 eV higher than for a 240 Volts discharge and appear consistent with the previous interpretation.

A faster ion current contribution is evidenced in a bump observed in the collector signal at 35 cm distance, and in an almost isolated peak at 70 cm. The corresponding velocity is 20 150 m/s, leading to a kinetic energy of 280 eV. The anode voltage, referred to ground, was only 230 Volts and is too low to lead to single charge Xe^+ ions of such high energy, even if wave-riding effects were taken into account. A significant contribution of double charge ions is well evidenced in the literature¹⁶ and the present contribution to ion current signal was attributed to Xe^{++} ions. In agreement with the above determination of the space potential seen by Xe^+ ions during their travel, the potential energy of Xe^{++} ions should be $2 \times 40 = 80$ eV and their total energy 360 eV. This total energy should be 400 eV if Xe^{++} and Xe^+ ions were born at the same plasma potential.

The uncertainty in the determination of Xe^{++} ions velocity is related to the uncertainty on their escaping time from the channel, of the order of 1 μs . The corresponding velocity uncertainty is 5%. It means that their total energy is at most 380 eV, indicating that double charge ions should be created at a plasma potential close to but smaller than single charge ions, with a plasma potential difference of 10-20 Volts.

The relative contribution of Xe^{++} ions in the plume, when derived from the two current contributions, appears a significant one : 15% for the local current density and 11 % for the ion flow density. In fact these contributions should be corrected by taking into account ion beam losses due to charge transfer collisions. For kinetic energies of 200 eV the charge exchange cross-section for Xe^+ ions and Xe^{++} ions¹⁶ are respectively 55 and 25 10^{-20} m^2 . The pressure in GREMI facility was $1,0 \cdot 10^{-4}$ mbar, corresponding to a xenon atom density of $2,4 \cdot 10^{18}$ m^{-3} . The mean free paths for charge exchange collisions is 0.75 m for Xe^+ ion and 1.6 m for Xe^{++} ions. The probabilities of a charge exchange collision on a travel distance of 70 cm are respectively 0.61 and 0.34 for Xe^+ and Xe^{++} ions. When taking into account these data, the Xe^{++} flow leaving the thruster, and observed at 70 cm on the plume axis, is reduced to 6% of the Xe^+ flux. The relative fraction of Xe^{++} ions in the HET's plume depends on thruster and operating conditions but the above data appear reasonable in comparison with other determinations¹⁷.

This interpretation of TOF data in terms of single charge and double charge ions seems correct, even if wave-riding effects, linked with space and time varying potentials can also accelerate ions but unlikely up to the energy level observed in our experiments.

V. Conclusion

A low power Hall Effect Thruster magnetic structure using exclusively permanent mini-magnets was designed and built at GREMI laboratory. The flexibility of the mini-magnet concept was used to evaluate three successive versions having the same magnetic topology but three values of magnetic field intensity. These tests showed that thermal constraints can be managed properly leading to a robustness of the magnetic concept. Thrust efficiencies referred to anodic Xenon flow are around 25 percent, lower than other ones reported in the literature at similar power levels. But they are considered as encouraging for future work if one considers that the mini-magnet flexibility was not used, up to now, for modifying the magnetic topology.

For similar xenon mass flow, the current/voltage characteristics obtained in the small size, rather high operating pressure, GREMI facility were not so far from those observed in the large, very low operating pressure, PIVOINE national research facility. But these two operating conditions differ significantly in various ways. While a current pulsating regime was always observed in GREMI conditions, rather quiet current fluctuating regimes were obtained in PIVOINE, and the plume divergence measured in GREMI conditions was significantly reduced.

These comparisons underline both the limits of the GREMI facility for thruster studies in this power range, with operating pressures up to $1.5 \cdot 10^{-4}$ mbar, and its interest in terms of cost and operating flexibility.

Time resolved data on the ion beam current, in GREMI pulsating regime, revealed time of flight effects assigned to the different velocities of single and double charge ion Xe ions. In spite of its coherence, further work is required for a definite conclusion on this interpretation of time of flight data : single charge ions with high kinetic energies could lead to similar TOF effects, but these ions have not been evidenced, up to now, with such high energies.

Finally, other physical studies, such as those concerning high frequency instabilities at 5-10 MHz, underline the general interest of physical insights acquired with such low power thrusters, independently of their possible interest for small satellite's technology.

Acknowledgments

The present work was achieved in the frame of the French national program GDR n°3161, "*Propulsion par Plasma dans l'espace*", supported by CNRS-CNES-SNECMA and Universities. A. Leufroy thank's CNES and regional authorities who support his PhD position. Two enginers from GREMI are especially acknowledged: J. Mathias who designed and built the PPI thruster, and B. Dumax who designed and tested electrical controls. The contribution of P. Lasgorceix, responsible of PIVOINE facility was essential for improvements of thrust balance required for this work and in leading PPI characterization campaigns. P.Renaudin is also gratefully acknowledged for helping in magnetic PPI transformations.

References

- ¹ M.Guyot, P. Renaudin, V. Cagan, C. Boniface, J-P. Bœuf, L. Garrigues, D. Pagnon, J. Mathias, A. Leufroy, T. Gibert, M. Dudeck « *New concepts for magnetic field generation in Hall Effect Hall Thrusters* », Proceedings of the Space Propulsion conference, paper 029, Heraklion 2008
- ² R. Koehne, F. Lindner, K.R. Schreitsmueller, H.G. Wicham, E. Zeyfang "Further investigations on low-density Hall accelerators", AIAA J., vol 8 N° 5, pp 873-879, May 1970
- ³ D. G. Courtney and Manuel Martinez-Sanchez, "Diverging Cusped-Field Hall Thruster (DCHT)" Paper IEPC-2007-39, Proceedings of the 30th International Electric Propulsion Conference, September 17-20, Firenze, Italy
- ⁴ G. Kornfeld, "Plasma Accelerator Arrangement" United States Patent 6,523,338 B1, 2003
- ⁵ P.Renaudin, V.Cagan, M.Guyot, A.Cadiou, P.Lasgorceix, M.Dudeck, V.Vial, P.Dumazert, "magnetic circuits for Hall thrusters, use of permanent magnets", Proceedings of the 28th International Electric Propulsion Conference, paper 284, March 17-21, 2003, Toulouse, France
- ⁶ J.C. Adam, J.P. Boeuf, N. Dubuit, M. Dudeck, L. Garrigues, D. Gresillon, A. Heron, G.J.M. Hagelaar, V. Kulaev, N. Lemoine, S. Mazouffre, J. Perez Luna, V. Pisarev, S. Tsikata, "Physics, simulation, and diagnostics of Hall Effect Thrusters", Plasma Physics and Controlled Fusion, 50 (2008) 124041 (17pp)
- ⁷ S. Mazouffre, A. Lazurenko, P. Lasgorceix, M. Dudeck, S. d'Escrivan, O. Duchemin, 2007, "Expanding frontiers: Towards high power Hall effect thrusters for interplanetary journeys", Proceedings of the 7th International Symposium on Launcher Technologies, 2007, Barcelona, Spain, paper O-25.
- ⁸ L. Albarede, T. Gibert, A. Lazurenko, A. Bouchoule "Laser injection of ultra-short electron bursts for the diagnosis of Hall thruster plasma" Plasma Sources Science and Technology, Vol 15, pp 805-817, 2006
- ⁹ D.H. Manzella, S. Oleson, J. Sankovic, T. Haag, A. Semenkin, V. Kim, "Evaluation of low power Hall thrusters propulsion", AIAA-96-2736, Joint Propulsion Conference, July 1996
- ¹⁰ A. Smirnov, Y. Raitses, N. J. Fish, "Parametric investigations of miniaturized cylindrical and annular Hall thrusters", Journal of Applied Physics, Vol 92, N° 10, 2002 pp 5673-5679
- ¹¹ A. Lazurenko, V. Vial, M. Prioul, and A. Bouchoule "Experimental investigation of high-frequency drifting perturbations in Hall thrusters", Physics of Plasmas, 12(1), 013501 (2005)
- ¹² S. Barral, K. Makowski, Z. Peradzynski, M. Dudeck, "Transit-time instability in Hall thrusters", Physics of Plasmas, Volume 12, Issue 7, pp. 073504-073504-9 (2005).
- ¹³ Y. V. Esipchuck and G. N. Tilinin, "Drift instability in a Hall-current plasma accelerator" Soviet Physics Technical Physics Vol 21 N°4, p417, 1976
- ¹⁴ A. Lazurenko, V. Krasnoselskikh, and A. Bouchoule "Experimental Insights into High-frequency Instabilities and Related Anomalous Electron Transport in Hall Thrusters", Transactions on Plasma Science, Special Issue, August 2008, TPS2078
- ¹⁵ M. Prioul, A. Bouchoule, S. Roche, L. Magne, D. Pagnon, M. Touzeau, P. Lasgorceix, "Insights on Physics of Hall Thrusters through Fast Current Interruptions and Discharge Transients", Paper IEPC-01-059, proceedings of the 27th International Electric Propulsion Conference, Pasadena, CA, 15-19 October 2001.
- ¹⁶ J. S. Miller, S. H. Pullins, D. J. Levandier, Y. Chiu, R. A. Dressler, "Xenon charge exchange cross sections for electrostatic thruster models", Journal of Applied Physics, Vol. 91, N° 3, 1 February 2002, pp 984-991
- ¹⁷ L. B. King and A. D. Gallimore, "Mass Spectral Measurements in the Plume of an SPT-100 Hall Thruster", Journal of Propulsion and Power, Vol. 16, No. 6, November–December 2000, p 1086-